IEEE Access
Multidisciplinary | Rapid Review | Open Access Journal

Received February 19, 2021, accepted April 5, 2021, date of publication April 23, 2021, date of current version May 17, 2021.

Digital Object Identifier 10.1109/ACCESS.2021.3075226

Automatic Recognition of Parathyroid Nodules in Ultrasound Images Based on Fused Prior Pathological Knowledge Features

YING WANG[1,2], LIN MAO[3], MING-AN YU[4], YING WEI[4], CAN HAO[1], AND DENGFENG DONG[1,2]

[1]Institute of Microelectronics of the Chinese Academy of Sciences, Beijing 100029, China
[2]School of Optoelectronics, University of Chinese Academy of Sciences, Beijing 100049, China
[3]First Research Institute of the Ministry of Public Security of China, Beijing 100048, China
[4]China-Japan Friendship Hospital, Beijing 100029, China

Corresponding author: Dengfeng Dong (dongdengfeng@ime.ac.cn)

This work was supported in part by the National Key Research and Development Program of China under Grant 2018YFB2003803, and in part by the Beijing University of Chemical Technology and China-Japan Friendship Hospital Joint Funding under Grant PYBZ1804.

ABSTRACT Automation diagnosis of parathyroid nodules is of crucial importance to recognize parathyroid nodules in ultrasound images. Aiming at the different nodule shapes of diverse patients, blurred boundaries, complex backgrounds and inhomogeneous intensity of ultrasound images, we propose a novel hybrid level set model to accurately segment nodules. The adaptive global term weight is determined based on the image local entropy of the region around the evolution contour and two scales are proposed for the local term to drive the evolution contour fast approaching to the boundary in order to avoid large amount of calculation and over-segmentation. We also propose membrane features and relative position features based on prior pathological knowledge to describe the inherent characteristics of parathyroid nodules different from thyroid and other nodules. We fused prior pathological knowledge features, morphology features and texture features of the segmented nodules to recognize parathyroid nodules by the support vector data description(SVDD). The experiment result indicates that the incorporation of the proposed hybrid level set segmentation method and the fused prior pathological knowledge features, morphology features and texture features improve the recognition accuracy and efficiency of parathyroid nodules, which is much higher than that only with morphology and texture features.

INDEX TERMS Parathyroid nodules, ultrasound images, hybrid level set, prior pathological knowledge, image local entropy, SVDD.

I. INTRODUCTION

Metabolism dysregulation of calcium and phosphorus is a common complication for chronic kidney disease (CKD) patients, which easily leads to secondary hyperparathyroidism (SHPT) [1] and seriously affects the life quality of patients. Therefore, it's necessary to remove the hyperplastic parathyroid nodules as early as possible [2].

Ultrasound-guided thermal ablation is gradually adopted to treat parathyroid nodules [3] with its advantages of precise positioning, minimally invasion and staged surgery. However, parathyroid nodules in ultrasound images have complex backgrounds accompanying around tissues and organs such as thyroids, tracheas and vessels. These tissues in ultrasound images are inhomogeneous and have no clear boundaries from other tissues. Furthermore, the locations, shapes and sizes of parathyroid nodules are diverse depending on different patients. Only the experienced experts can diagnose parathyroid nodules from thyroid nodules and lymph nodules accurately.

Currently deep learning is widely used to recognize objects. However the noises in ultrasound images are serious and the boundaries between different tissues are blurry, so the extracted object features by the network are not obvious from other tissues and the tissue recognition accuracy is not satisfied. Although some networks [4], [5] are used to improve the image quality, the recognition accuracy is also not satisfied for the ultrasound images with complex

The associate editor coordinating the review of this manuscript and approving it for publication was Jiachen Yang.

backgrounds. Further it is difficult to get large parathyroid ultrasound images marked by the experienced experts. Therefore, automatic recognition of parathyroid nodules in ultrasound images based on machine learning is a better solution. This method mainly includes three steps: suspected parathyroid nodules segmentation, features extraction and parathyroid nodules recognition.

Traditional segmentation methods such as threshold methods and regional growth algorithms exhibit excellent effects to objects with high contrast and homogeneous intensity. However it is unsatisfied to parathyroid nodules segmentation in ultrasound images because of the heavy noises, blurry boundaries and complex backgrounds. At present, researchers have tried to apply fuzzy theory [6], neural network [7] and active contour model [8] to segment objects with inhomogeneous intensity and complex backgrounds in images. The level set method as one of the active contour models embeds two dimensional contours into the higher dimensional surfaces and transfers the segmentation problem to the solving of partial differential equations. These characteristics make the level set method suitable to segment parathyroid nodules in ultrasound images. Chan-Vese(CV) model segments objects [9] based on global information, however there is over segmentation or under segmentation when intensity is inhomogeneous. Region Scale Fitting(RSF) model is adaptable to segment objects when intensity is inhomogeneous based on local information [10], however it is sensitive to the initial contour position and easily falls into local minimum. Reference [11] gets better results for the most real and simulation medical images when boundaries are clear. Aiming to the blurry boundaries between tissues, inhomogeneous intensity of parathyroid nodules and heavy noises in ultrasound images, this study proposes a hybrid level set model to improve the segmentation accuracy and adaptability to diversiform parathyroid nodules by fully using global and local intensity information in images.

Morphology features describe the shape and the boundary contour of objects, and texture features describe inner echo mode characteristics of tissues in ultrasound images. So they are widely used to recognize tissues or organs in ultrasound images. Zhang *et al.* [12] recognized benign ormalignant of lymph nodes by boundaries regularity, sharpness, similarity to the circle and texture based on inner echo modes. Thyroid texture features were extracted by using wavelet transformation and Gabor transformation in references [13], [14] to recognize benign or malignant thyroid nodules in ultrasound images. Due to low contrast between parathyroid nodules and backgrounds, diverse shapes of parathyroid nodules and heavy noises, the features difference between parathyroid nodules, thyroid nodules or lymph nodes in ultrasound images is not obvious. Therefore it is difficult to distinguish parathyroid nodules only using morphology features and texture features.

Aiming to the highly inhomogeneous intensity, heavy noises and diverse parathyroids in ultrasound images, an adaptive hybrid level set model based on the image local entropy is proposed to segment nodules. We also propose the features of highlight membranes, relative positions between parathyroid nodules and thyroids which are inherent characteristics of parathyroid nodules different from other nodules based on prior pathology knowledge to improve the recognition accuracy of parathyroid nodules. The main ideas in this paper are: (a) The suspected parathyroid nodule is accurately segmented by the proposed hybrid level set model based on the image local entropy, then (b) the prior knowledge features of the segmented nodule are extracted and described, and finally (c) the parathyroid nodule in the ultrasound images provided by an interventional ultrasound department of a hospital is recognized by the fused features.

II. SEGMENTATION OF PARATHYROID NODULES BY THE HYBRID LEVEL SET MODEL USING IMAGE LOCAL ENTROPY

The segmentation accuracy of nodules is the precondition to accurately recognize parathyroid nodules. Inhomogeneous intensity, diverse shapes and blurred boundaries of parathyroid nodules bring great challenges to accurate segmentation of parathyroid nodules in ultrasound images. The improved CV model [15] based on global information has fast convergence speed, however parathyroid nodules are often undersegmented by only using global information. The fixed weight model [16] easily falls into the local minimum when intensity around the nodules is inhomogeneous, which is not adaptive to parathyroid ultrasound images. In this paper we proposed a hybrid level set model aiming to accurately segment nodules with complex backgrounds and inhomogeneous intensity in ultrasound images by adjusting the model weight adaptively.

The adaptive hybrid level set for segmentation of suspected nodules in ultrasound images consists of two main parts as shown in Fig. 1. The initial contour of the suspected nodule is determined by the marked points and the image local entropy is calculated as the global term weight. First, the global term dominates the evolution curve fast converging to the boundary and the large scale is used for the local term. Secondly, the local term dominates the evolution when the evolution curve is near to the boundary. When the change of evolution curve is smaller than the threshold, the smaller scale is used and makes the curve accurately stop at the real boundary.

A. THE HYBRID LEVEL SET MODEL

$I : \Omega \to \Re$ is an intensity image, the energy function of the CV level set model is:

$$E^{\mathrm{CV}}(C, c_1, c_2) = \lambda_1 \int_{\Omega_1} |I(x) - c_1|^2 \mathrm{d}x + \lambda_2 \int_{\Omega_2} |I(x) - c_2|^2 \mathrm{d}x \tag{1}$$

where $I(x)$ is the intensity of the point x, contour C is the zero level set of the level set function ϕ. C separates Ω into the inside region Ω_1 and the outside region Ω_2 corresponding to the object and the background respectively. c_1 and c_2 are the mean intensities of Ω_1 and Ω_2, λ_1 and λ_2 are non-negative constants.

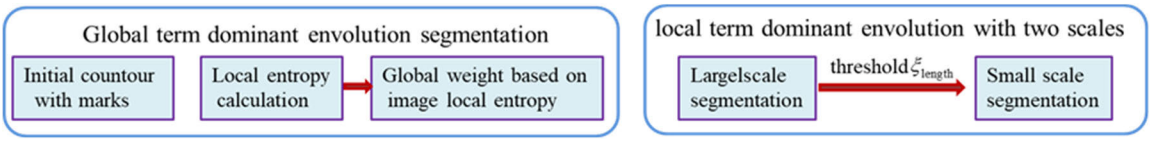

FIGURE 1. Flow chart of segmentation based on the hybrid level set model.

Based on the variational method and gradient descent principle, we get the partial differential equation (2) of the CV model by substituting the level set function ϕ [9] into the formula (1):

$$\frac{\partial \phi}{\partial t} = \delta_\varepsilon[-\lambda_1(I-c_1)^2 + \lambda_2(I-c_2)^2] \tag{2}$$

c_1, c_2 are calculated by formula (3):

$$\begin{cases} c_1 = \dfrac{\int_\Omega I(x)H_\varepsilon(\phi)\mathrm{d}x}{\int_\Omega H_\varepsilon(\phi)\mathrm{d}x} \\ c_2 = \dfrac{\int_\Omega I(x)(1-H_\varepsilon(\phi))\mathrm{d}x}{\int_\Omega (1-H_\varepsilon(\phi))\mathrm{d}x} \end{cases} \tag{3}$$

where $H_\varepsilon(\phi), \delta_\varepsilon(\phi)$ are the smoothed Heaviside function and the smoothed Dirac delta function respectively.

The energy function of RSF model is:

$$E^{\mathrm{RSF}}(C,f_1,f_2) = \lambda_1 \iint_{\Omega_1} K_\sigma(x-y)\,|I(y)-f_1(x)|^2 \mathrm{d}y\mathrm{d}x + \lambda_2 \iint_{\Omega_2} K_\sigma(x-y)\,|I(y)-f_2(x)|^2 \mathrm{d}y\mathrm{d}x \tag{4}$$

where K_σ is Gaussian function, its size is controlled by the standard deviation σ. The point x is the center of the local region $I(y)$. $f_1(x), f_2(x)$ are the approximate intensities of Ω_1 and Ω_2, which are calculated by formula (5):

$$\begin{cases} f_1 = \dfrac{K_\sigma * (H_\varepsilon(\phi)I(x))}{K_\sigma * H_\varepsilon(\phi)} \\ f_2 = \dfrac{K_\sigma * ((1-H_\varepsilon(\phi))I(x))}{K_\sigma * (1-H_\varepsilon(\phi))} \end{cases} \tag{5}$$

The partial differential equation of the RSF model is:

$$\frac{\partial \phi}{\partial t} = -\delta_\varepsilon(\phi)\,(\lambda_1 e_1 - \lambda_2 e_2) \tag{6}$$

where e_1, e_2 are calculated by formula (7):

$$\begin{cases} e_1 = \int K_\sigma(y-x)\,|I(x)-f_1(y)|^2\,\mathrm{d}y \\ e_2 = \int K_\sigma(y-x)\,|I(x)-f_2(y)|^2\,\mathrm{d}y \end{cases} \tag{7}$$

The proposed hybrid level set model in this paper consists of the global term of the improved CV model [15], the local term of the RSF model, the length term $L(\varphi) = \int_\Omega \delta_\varepsilon(\varphi)\,|\nabla\varphi| dx$ and the penalty term $P(\varphi) = \frac{1}{2}\int_\Omega (|\nabla\varphi - 1|)^2 dx$.

Its partial differential equation is as formula (8):

$$\frac{\partial \phi}{\partial t} = \alpha \cdot \left(\delta_\varepsilon(\phi)(I - \frac{c_1+c_2}{2})\right) + \beta \cdot (-\delta_\varepsilon(\phi)\,(\lambda_1 e_1 - \lambda_2 e_2)) + \nu \cdot \delta_\varepsilon(\phi) div\left(\frac{\nabla\phi}{|\nabla\phi|}\right) + \mu \cdot \left(\nabla^2\phi - div\left(\frac{\nabla\phi}{|\nabla\phi|}\right)\right) \tag{8}$$

α is the weight of the global term, β is the weight of the local term. ν, μ are the coefficients of the length term and the penalty term respectively, which make the contour smooth during evolution.

B. ADAPTIVE WEIGHT OF THE GLOBAL TERM BASED ON IMAGE LOCAL ENTROPY

The global term of the hybrid level set model fully utilizes global information in images to move the evolution contour to the object boundary. Because the image local entropy presents the local intensity distribution, it is used to adaptively determine the weight of the global term based on the fact that the farther the curve is to the object boundary, the more homogenous the intensity around the curve region is, the smaller the image local entropy is accordingly. If the image size is $M \times N$, the size of the window centered the point (i,j) is $m \times n$, n'_l is the pixels number of the intensity l in the window centered the point (i,j), the probability p'_l of l is $P'_l = \frac{n'_l}{m\times n}$. The local entropy of the point (i,j) is $h(i,j) = -\sum_{l=0}^{L-1} P'_l(i,j)\log P'_l(i,j), L = 1, 2 \ldots .256$. We use the image local entropy as the weight of the global term in the hybrid level set model. The weight of the global term is defined as:

$$\alpha = \begin{pmatrix} \alpha_{11} & \cdots & \alpha_{1N} \\ \vdots & \alpha_{ij} & \vdots \\ \alpha_{M1} & \cdots & \alpha_{MN} \end{pmatrix}, \quad \alpha_{ij} = e^{-h(i,j)}, \quad 1 \le i \le M, \quad 1 \le j \le N \tag{9}$$

When the contour locates in the homogeneous intensity region, the image local entropy is small and the weight of the global term is large based on formula (9). The global term is dominant and drives the curve quickly approaching to the target boundary. Generally when the contour is near to the boundary, the intensity around the boundary is inhomogeneous and the weight of the global term becomes smaller, so the local term is dominant and makes the contour accurately approaching to the target boundary.

Compared with the fixed weight model, the image local entropy adjusts the weight of the global term adaptively based on the intensity distribution around the evolution curve. The driving force of the contour by the hybrid level set model is more adaptable to the diverse parathyroid nodules in ultrasound images.

The size of the local term scale depends on the standard deviation of Gaussian function, which affects the calculation

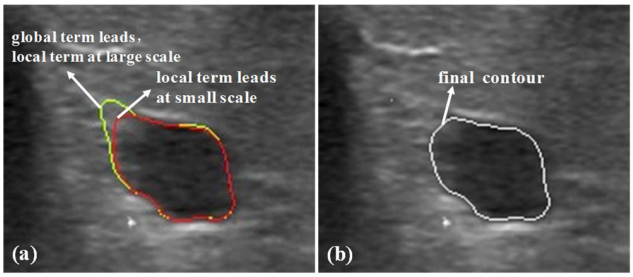

FIGURE 2. The contour evolution by the proposed hybrid level set model. (a) The contours dominated by global and local terms with two scales (b) The convergence curve to the nodule boundary.

amount and evolution speed of the contour. When the scale is large, it cannot fall into local minimum as the small scale does, however the object is easily over-segmented when the contour is very near to the boundary and the large amount calculation leads to the slow evolution speed. In order to avoid this situation, two scales are proposed for the local term. When the contour is a little far away from the object boundary a larger scale is adopted to make the contour fast closing to the object boundary, and when the contour is very near to the object boundary, a smaller scale is adopted to make the curve stopping at the nodule boundary accurately.

A threshold ξ_{length} corresponding to the contour length change is set. If the contour length change between two consecutive iterations is less than the ξ_{length} within a certain number of iterations, the contour is considered to be very near to the object boundary, the larger scale is instead by the smaller scale. ξ_{length} is determined by the empirical value, which are normally 3 to 5 pixels.

Figure 2 gives the segmented nodule by the hybrid level set. When the contour was far away from the nodule boundary, it located in the homogeneous intensity region. The global term weight was larger and dominated the contour approaching to the boundary and the larger scale was used for the local term, which was shown as the yellow curve in Fig.2(a). When the contour was near to the nodule boundary it located in the inhomogeneous intensity region, the local term with the smaller scale dominated the contour accurately converging to the nodule boundary, which was shown as the white curve in Fig. 2(b).

C. SEGMENTED PARATHYROID NODULES IN ULTRASOUND IMAGES BASED ON THE HYBRID LEVEL SET MODEL

Four nodules surrounded by tissues with different intensity distributions in ultrasound images were selected as shown in Fig. 3. The boundary of the nodule in Fig. 3(a) is relatively distinct, only part boundary of the nodule is blurry in Fig.3(b), the nodule boundary in Fig.3(c) is all blurry and the nodule in Fig.3(d) connects to the vessel. These four ultrasound images represent typical connection situations with other tissues in the region around the nodule boundaries.

The hybrid level set model proposed in this paper, the improved CV model [15] and the fixed weight model [16] were used to segment four nodules in Fig.3 to compare the segmentation accuracy for different parathyroid ultrasound images. The segmentation results are shown in Fig. 4.

The first column of Fig.4 gives the initial irregular quadrangle contours obtained by four marks connected in turn. The second column to the fourth column are the segmented nodules by the improved CV model, the fixed weight model and the proposed adaptive hybrid level set model respectively. The nodules were under-segmented or over-segmented because of only using the global information of images based on the improved CV model. The nodules with clear boundaries were accurately segmented by the fixed weight model, but there were improper segmentation for nodules with blurry boundary or nodules connecting to the vessels as shown in the third and fourth rows. The fourth column was segmented nodules by our hybrid level set model, which all nodules with different intensity distributions and tissues around were accurately segmented. We simply set irregular quadrangles as initial contours, the shapes of initial contours can also be ovals, which scarcely has effect to the final segmented boundaries.

Dice similarity coefficient(DSC) [17], iterations and running time were used to quantitatively compare the segmentation results by these three models in Table 1. The DSC of the adaptive hybrid model is higher than that of the two other models, while the iterations and running time are less than that of the two other models. It both owed to the adaptive global item weight based on the image local entropy and the two-scale local term of the hybrid model which made the contours converging to the boundary accurately and also decreased the calculation amount and iterations. The accuracy of the segmented nodules was also verified by the imageological experts who gave the initial marks of nodules. The accurate segmentation result is very important and helpful to diagnose parathyroid nodules.

III. FEATURE EXTRACTION AND DESCRIPTION OF PARATHYROID NODULES BASED ON PRIOR KNOWLEDGE

Although the shapes of thyroid, parathyroid and lymph are different, they are all nearly diverse ovals depending on patients. The texture of thyroid nodules and lymph is inhomogeneous while parathyroid nodules are mostly homogeneous in ultrasound images. However there is not distinct texture difference due to noises and low contrast between the parathyroid gland nodules and complex backgrounds. Therefore the recognition accuracy of parathyroid nodules only with morphology and texture features is not satisfied. In this paper we try to find the inherent features of parathyroid nodules different from thyroid and lymph glands based on the prior pathological knowledge to improve the recognition accuracy.

A. PRIOR PATHOLOGICAL KNOWLEDGE FEATURES

Based on pathological analysis, there is a membrane between the parathyroid gland and the thyroid gland. When parathyroid glands proliferate to form nodules, the membranes

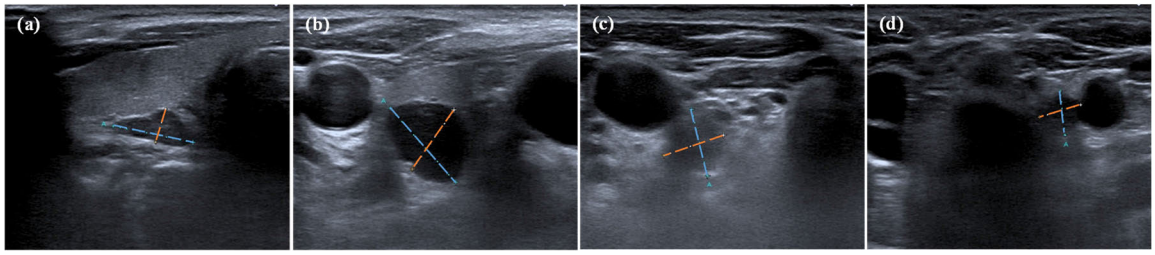

FIGURE 3. Nodules in parathyroid ultrasound images with different intensity distribution.

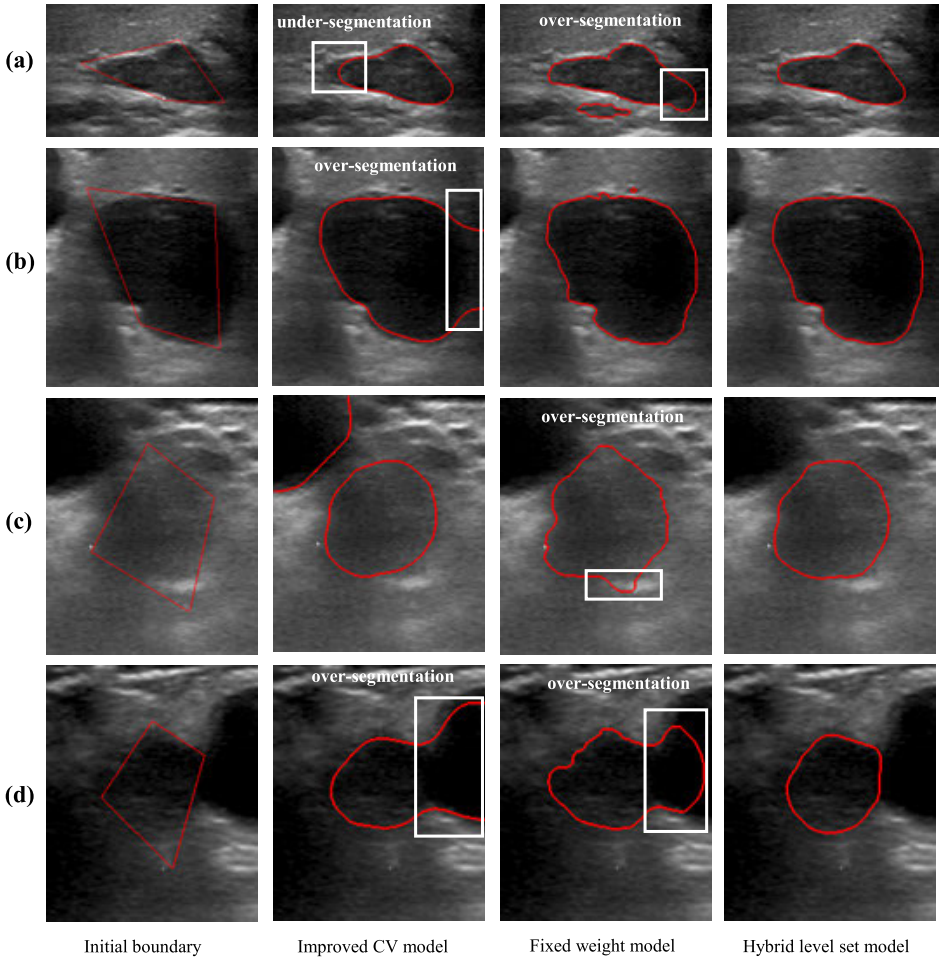

FIGURE 4. Nodules segmentation results by three level set models.

TABLE 1. Evaluation of nodules segmented by the three level set models.

parathyroid ultrasound images	Improved CV model			Fixed weight model			Proposed hybrid model		
	DSC	iterations	running time/s	DSC	iterations	running time/s	DSC	iterations	running time/s
a	0.91	846	413.94	0.85	477	211.54	0.95	258	127.74
b	0.72	1000	727.54	0.97	1000	676.31	0.98	996	633.97
c	0.81	670	452.68	0.91	704	434.31	0.92	263	201.14
d	0.81	1000	343.30	0.78	1000	339.06	0.93	380	175.68

between thyroid glands and parathyroid glands are compressed by parathyroid nodules and the high-level echo corresponding to the bright area is detected in ultrasound images. There is no membrane around the thyroid nodule because it is inside the thyroid gland. Most areas around thyroid nodules are thyroid tissues while the parathyroid gland normally locates behind the thyroid gland. There is only part of the thyroid tissue bordering with the parathyroid nodule.

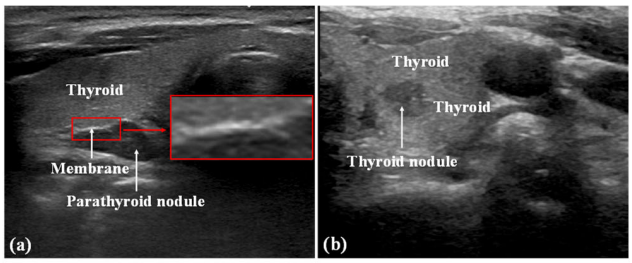

FIGURE 5. Membranes and relative positions between suspected nodules and thyroid glands in ultrasound images, (a) the parathyroid nodule and (b) the thyroid nodule.

Figure 5(a) is a parathyroid nodule. There is the membrane between the thyroid and the parathyroid nodule, the red rectangle in the right is its enlarged view. Only the region outside the upper boundary of the parathyroid nodule is the thyroid tissue. A thyroid nodule is inside the thyroid and there is no membrane as Fig.5(b) shown. Nearly all regions outside the thyroid nodule are thyroid tissues, such as its up, right, and bottom. Therefore, bright membrane features and the position features relative to the thyroid based on pathological characteristics are used to recognize parathyroid nodules.

B. EXTRACTION AND DESCRIPTION OF MEMBRANE FEATURES

The membrane is located in the outer boundary of the parathyroid nodule. The outer annular area of the segmented nodule in Section II is extracted by morphological expansion. The process of membrane extraction in the annular area is as follows:

1) The bright area is extracted by the intensity threshold determined by the maximum entropy algorithm and its maximum connected region is selected as the rough region of the membrane.

2) The improved region growing algorithm is used to get the accurate suspected membrane region. First the pixel with the maximum intensity in the rough region is selected as the initial seed point, and then eight neighborhoods of the seed point are traversed to decide whether each traversal pixel belongs to the suspected membrane. If so, it is assigned as the new seed, and the above step is repeated until no suspected membrane pixels can be found. Formula (10) gives the criteria.

$$\left|x_p - X_{aver}\right| \leq T \tag{10}$$

where x_p is the intensity of the traversed pixel, X_{aver} is the mean intensity of the current suspected membrane. T is the region growing threshold and is determined by:

$$T = \sqrt{\frac{1}{m}\sum_{j=1}^{m}(x_j - E(x))^2} \tag{11}$$

where $E(x) = \frac{1}{m}\sum_{j=1}^{m} x_j$ is the average intensity of the rough region, m is the number of total pixels in the rough region, x_j is the intensity of the pixel in the rough membrane region.

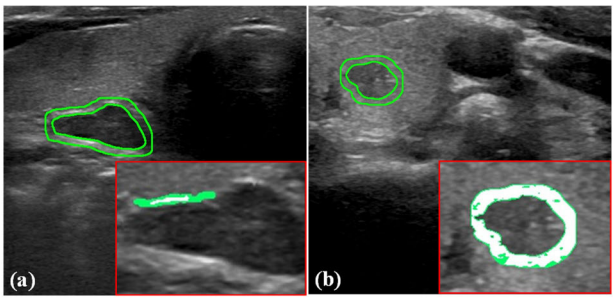

FIGURE 6. Membrane extraction (a) the extracted membrane of the parathyroid nodule (b) the extracted bright region of the thyroid nodule.

Figure 6 gives the extracted annular of the suspected parathyroid nodules dotted by the green curves. The white region in the annular is the extracted suspected membrane, the red rectangle is the enlarged view of the extracted suspected membrane. The membrane length in Fig.6(a) is shorter than that of the thyroid nodule in Fig.6(b) because there is no membrane between the thyroid nodule and the thyroid. Therefore the length feature of the membrane is used to recognize parathyroid nodules. The membrane is above the parathyroid nodule because the parathyroid gland is generally behind the thyroid gland. So the relative position between the extracted suspected membrane and the suspected nodule is also used to distinguish parathyroid nodules. The membrane features are described as follows:

(1) Length L_{en} is the distance between the two end points of the membrane along the horizon direction as shown in Fig.7. If L_{en} is short, the suspected area is the membrane.

(2) Relative position is described by θ,, which is the angle from the horizon line passing the nodule centroid to the line connecting the suspected membrane centroid to the nodule centroid along counterclockwise. If there is the membrane, $sin\theta > 0$, or $sin\theta < 0$. The centroids of the nodules and the suspected membranes are calculated by formula 12.

$$\begin{cases} x_c = \dfrac{\sum\limits_{m} x_i}{m} \\ y_c = \dfrac{\sum\limits_{m} y_i}{m} \end{cases} \tag{12}$$

where m is the number of total pixels of the segmented nodule or the suspected membrane. x_i , y_i are the coordinate of the pixel in the segmented nodule or the suspected membrane.

C. THE RELATIVE POSITION FEATURES BETWEEN THE NODULE AND THE THYROID

Only part thyroid tissues are outside the parathyroid nodule while thyroid tissues nearly surround the thyroid nodule. The thyroid tissue in ultrasound images is bright and its texture is homogenous as shown in Fig.5. So texture homogeneity and brightness are used to distinguish whether the tissue outside the segmented nodule is thyroid.

Lacunarity is used to quantify the texture homogeneity. First the minimum enclosing rectangle of the outer annular in Section III-B is obtained, which its two sides are along

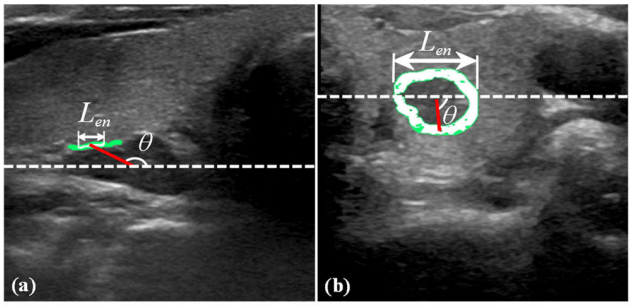

FIGURE 7. The length and the relative position features of the membrane (a) the parathyroid nodule and (b) the thyroid nodule.

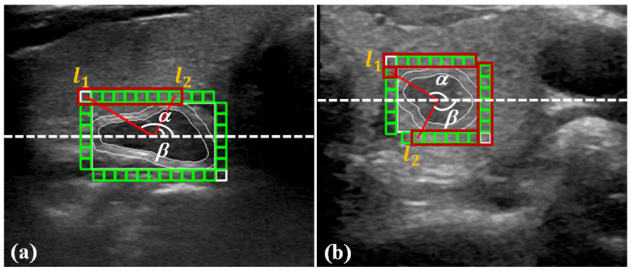

FIGURE 8. Relative position features between the nodule and the thyroid tissue (a) the parathyroid nodule (b) the thyroid nodule.

the horizontal and vertical direction respectively. Then this rectangle is divided into several small squares, for example each of which is 16×16 pixels. Box Column Mean(LBCM) method [18] is used to calculate lacunarity in order to estimate the intensity homogeneity of each small square. The lacunarity calculation details are as follows:

(1) A box with the size of $r \times r$ is used to traverse each small square. The average intensity of the area covered by the box is defined as mass M. n_M is the number of boxes with the mass M. N is the total sliding number of the box within the small square.

(2) The probability of the sliding boxes with the mass M is $q(M) = \frac{n_M}{N}$. The first moment and the second moment of the probability distributions are calculated as follows:

$$Z_1 = \sum Mq(M) \tag{13}$$

$$Z_2 = \sum M^2 q(M) \tag{14}$$

(3) The lacunarity value Λ of each small square is calculated as follows:

$$\Lambda = \frac{Z_2}{(Z_1)^2} \tag{15}$$

A is the mean intensity of the small square, the average intensity threshold is $A_{th} = 70$. The lacunarity threshold $\Lambda_{th} = 1.0121$, Λ_{th} is determined by Mann-Whitney U test of lacunarity of all small squares. If Λ and average intensity A demand $\Lambda \leq \Lambda_{th}$ and $A \geq A_{th}$, the small square is considered as the thyroid tissue. However some small squares are probably misjudged as the non-thyroid tissue due to noises in ultrasound images. Aiming to this status, if the two sides of the no-thyroid small square are thyroid tissues, this small square is redetermined as the thyroid tissue.

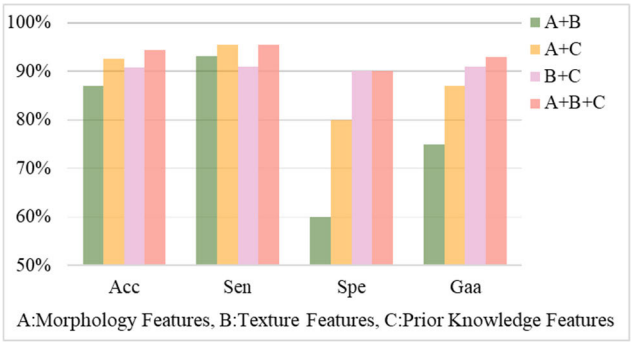

FIGURE 9. The recognition result of bar graph with different fusion features.

Figure 8 gives the detected result shown as green and white boxes. The small squares in the red rectangles are thyroid tissues. Only a few small squares in the upper parathyroid nodule are thyroid tissues as Fig.8(a) shown, while most small squares around the thyroid nodule are thyroid tissues as Fig.8(b) shown. Therefore features of the thyroid lengths L_{th} around the nodules and the relative positions between the nodules and the thyroid tissues are used to describe the relative position. The relative position features are as follows:

(1) The thyroid length L_{th} is the ratio of the number of small squares detected as thyroid to the number of all small squares;

(2) Relative position between the nodule and the thyroid: the horizontal line passes through the nodule centroid, the line l_1 connects the nodule centroid and the center of the first thyroid small square, the line l_2 connects the nodule centroid and the center of the end thyroid small square, α, β are the angles from the horizion line to l_1 and the horizon line to l_2 counterclockwise respectively as shown in Fig.9. If $\sin\alpha + \sin\beta$ is larger the suspected nodule is the parathyroid nodule. If $\sin\alpha + \sin\beta$ is smaller or negative the nodule is the thyroid nodule.

D. MORPHOLOGY FEATURES AND TEXTURE FEATURES OF NODULES

Thyroid nodules are generally round or oval and lymph nodes are generally oblong. Unlike thyroid and lymph most parathyroid nodules are irregular. The more irregular the nodules are, the more likely the parathyroid nodules are. Because there are multiple echo modes such as strong echo, isoecho or mixed echo for thyroid nodules, the texture of thyroid nodules is inhomogeneous. Parathyroid nodules are mostly corresponding to low echoes, their textures are homogeneous in ultrasound images. Five morphology features including aspect ratio, compactness, standard deviation of normalized radial length [19], acutance [20] and edge intensity variation [12] are used to distinguish the nodules irregularity and clarity of boundaries. Twelve texture features including energy, entropy, contrast, correlation, deficit moment, variance, sum average, sum variance, sum entropy, difference average, difference variance and difference entropy based on gray co-occurrence matrix are used to clarify the thyroid nodules, lymph nodes or parathyroid nodules. Principle component

TABLE 2. Recognition accuracy of four different fused features by SVDD.

Fusion Feature	Acc/%	Sen/%	Spe/%	Gaa/%
A+B	87.04	93.18	60.00	75.77
A+C	92.59	95.45	80.00	87.38
B+C	90.74	90.91	90.00	91.45
A+B+C	94.44	95.45	90.00	92.68

A:MorphologyFeatures, B: Texture Features, C: Prior Knowledge Features

analysis (PCA) is used to remove redundant information of texture features and only two dimensions are reserved by the 95% contribution.

IV. PARATHYROID NODULES RECOGNITION RESULT BASED ON FUSION FEATURES AND SVDD

Support vector machine is commonly used to recognize two classes or multiple classes and it is excellent only when the numbers of various class samples are equivalent. The recognition of parathyroid nodules from thyroid nodules or lymph nodes is the single classification so the samples of parathyroid nodules are much larger than that of non-parathyroid nodules. The support vector data description (SVDD) [21] is selected to recognize parathyroid nodules because of its prominent manifestation in unbalanced samples and single classification [22].

The recognition accuracy of parathyroid nodules is unsatisfied only with morphology and texture features because of low contrast between nodules and backgrounds, heavy noises and diverseness of patients in ultrasound images. Membrane features and relative position features describe pathological characteristics of parathyroid nodules different from other nodules so they are robust to noises and complicated backgrounds in ultrasound images. Therefore these prior pathological knowledge features fused with morphology and texture features are used to recognize parathyroid nodules.

There were 414 training ultrasound images provided by an interventional ultrasound department of the hospital, which included 404 images of parathyroid nodules and 10 images of non-parathyroid nodules. 404 parathyroid nodules images were divided into 10 groups by 10-fold cross-processing, 9 groups of which were selected as training set of SVDD, the remaining group and 10 images of non-parathyroid nodules were selected as the test set to construct the optimal hypersphere model of SVDD. Considering the imbalance samples of parathyroid and thyroid, accuracy (Acc), sensitivity (Sen), specificity (Spe) [23] and geometric average accuracy (Gaa) [24] were used to evaluate parathyroid nodules recognition results.

Based on the constructed optimal hypersphere model of SVDD, another 44 parathyroid ultrasound images and 10 non-parathyroid ultrasound images were verified. We used four groups of different fusion features to recognize parathyroid nodules. The first group was morphology and texture features, the second group was morphology and prior knowledge features, the third group was texture and prior knowledge features, the fourth group was morphology, texture and prior knowledge features. The recognition results are shown in Table 2 and Fig. 9. It can be seen that it has higher recognition accuracy with the fused three features of prior knowledge features, morphology features and texture features than that for only two kinds of features. Also the Sen for the parathyroid nodules recognition, the Spe for non-parathyroid nodules recognition and the Gaa for recognition reliability are higher with the fused three features than that for only two kinds of features.

V. CONCLUSION

Inhomogeneous intensity, different nodule shapes of diverse patients and the blurred boundaries between nodules and backgrounds bring great challenges to automatic segmentation and recognition of parathyroid nodules by ultrasound images. To improve the segmentation efficiency and accuracy, we proposed the hybrid level set model to segment nodules in ultrasound images. The global term weight was adaptively adjusted based on the image local entropy depending on the intensity distribution around the evolution curve. In order to avoid large amount of calculation and over-segmentation, two scales were proposed for the local term of the hybrid level set. Based on our proposed hybrid level set model all nodules can be segmented accurately and efficiently. In order to improve the recognition accuracy, we proposed prior pathological knowledge features of membrane features and relative position features to describe the inherent characteristic of parathyroid nodules different from other nodules, which are robust to noises and complicated backgrounds. The fusion features of morphology features, texture features and prior knowledge features were used to recognize parathyroid nodules based on SVDD. We segmented nodules in the ultrasound images with our hybrid level set model and recognized the parathyroid nodules with fusion features. The experiment results show that the recognition accuracy was increased to 94.44%, which is much higher than that only with morphology features and texture features.

REFERENCES

[1] S.-J. Hwang, M.-Y. Lin, and H.-C. Chen, "Prevalence of chronic kidney disease in China," *Lancet*, vol. 380, no. 9838, p. 213, Jul. 2012.
[2] A. L. E. Cancela, R. B. Oliveira, F. G. Graciolli, L. M. dos Reis, F. Barreto, D. V. Barreto, L. Cuppari, V. Jorgetti, A. B. Carvalho, M. E. Canziani, and R. M. A. Moysés, "Fibroblast growth factor 23 in hemodialysis patients: Effects of phosphate binder, calcitriol and calcium concentration in the dialysate," *Nephron Clin. Pract.*, vol. 117, no. 1, pp. c74–c82, 2011.
[3] J.-Q. Zhang, M. Qiu, J.-G. Sheng, F. Lu, L.-L. Zhao, H. Zhang, and Z.-P. Diao, "Ultrasound-guided percutaneous thermal ablation for benign parathyroid nodules," *Academic J. 2nd Mil. Med. Univ.*, vol. 33, no. 4, pp. 362–370, Nov. 2013.
[4] X. Yang, X. Jiang, L. Zhou, Y. Wang, and Y. Zhang, "Active contours driven by local and global region-based information for image segmentation," *IEEE Access*, vol. 8, pp. 6460–6470, 2020.

[5] J. Fang, H. Liu, L. Zhang, J. Liu, and H. Liu, "Region-edge-based active contours driven by hybrid and local fuzzy region-based energy for image segmentation," *Inf. Sci.*, vol. 546, pp. 397–419, Feb. 2021.
[6] T. O. Oladele, C. D. Okonji, A. Adekanmi, and F. F. Abiola, "Neuro-fuzzy expert system for diagnosis of thyroid diseases," *J. Ann. Comput. Sci. Ser.*, vol. 16, no. 2, pp. 45–54, 2018.
[7] M. Malathi and S. Srinivasan, "Classification of ultrasoud thyroid nodule using feed forward neural network," *J. Asian J. Res. Social Sci. Humanities*, vol. 7, no. 2, pp. 475–482, 2017.
[8] W. Du and N. Sang, "An effective segmentation method of ultrasonic thyroid nodules," *Proc. SPIE*, vol.9814, Dec. 2015, Art. no. 98140F.
[9] T. F. Chan and L. A. Vese, "Active contours without edges," *IEEE Trans. Image Process.*, vol. 10, no. 2, pp. 266–277, Feb. 2001.
[10] C. Li, C.-Y. Kao, J. C. Gore, and Z. Ding, "Minimization of region-scalable fitting energy for image segmentation," *IEEE Trans. Image Process.*, vol. 17, no. 10, pp. 1940–1949, Oct. 2008.
[11] S. Zhang and F. He, "DRCDN: Learning deep residual convolutional dehazing networks," *Vis. Comput.*, vol. 36, no. 9, pp. 1797–1808, Sep. 2020.
[12] J. Zhang, Y. Wang, Y. Dong, and Y. Wang, "Sonographic feature extraction of cervical lymph nodes and its relationship with segmentation methods," *J. Ultrasound Med.*, vol. 25, no. 8, pp. 995–1008, Aug. 2006.
[13] A. A. Ardakani, A. Gharbali, and A. Mohammadi, "Classification of benign and malignant thyroid nodules using wavelet texture analysis of sonograms," *J. Ultrasound Med.*, vol. 34, no. 11, pp. 1983–1989, Nov. 2015.
[14] U. R. Acharya, P. Chowriappa, H. Fujita, S. Bhat, S. Dua, J. E. W. Koh, L. W. J. Eugene, P. Kongmebhol, and K. H. Ng, "Thyroid lesion classification in 242 patient population using Gabor transform features from high resolution ultrasound images," *Knowl.-Based Syst.*, vol. 107, pp. 235–245, Sep. 2016.
[15] K. Zhang, W. G. Zhou, Z. Zhang, and X. J. Zheng, "Improved C–V active contour model," *J., Opto-Electron. Eng.*, vol. 35, no. 12, pp. 112–116, 2008.
[16] L. Zhou, P. Li, and X. Ren, "An improved image segmentation active contour model," *J., Comput. Appl. Softw.*, vol. 30, no. 8, pp. 184–186, 2013.
[17] T. Dietenbeck, M. Alessandrini, D. Friboulet, and O. Bernard, "Creaseg: A free software for the evaluation of image segmentation algorithms based on level-set," in *Proc. IEEE Int. Conf. Image Process.*, Sep. 2010, pp. 665–668.
[18] G. Ji and Z. Yu, "Synergy between fractal dimension and lacunarity discriminating liver from ultrasonic images," *J. Comput. Eng. Appl.*, vol. 49, no. 2, pp. 211–218, 2013.
[19] J. Zhao and Y. Qi, "A novel feature extraction algorithm of thyroid tumor ultrasound image," *J., Opto-Electron. Eng.*, vol. 40, no. 9, pp. 8–15, 2013.
[20] L. Li, *Study on Feature Extraction and Classification Algorithm of Thyroid Nodules*. Changchun, China: Changchun Univ. Technology, 2018.
[21] D. M. J. Tax and R. P. W. Duin, "Support vector data description," *Mach. Learn.*, vol. 54, no. 1, pp. 45–66, Jan. 2004.
[22] V. Mygdalis, A. Iosifidis, A. Tefas, and I. Pitas, "Semi-supervised subclass support vector data description for image and video classification," *Neurocomputing*, vol. 278, pp. 51–61, Feb. 2018.
[23] Y. N. Hwang, J. H. Lee, G. Y. Kim, Y. Y. Jiang, and S. M. Kim, "Classification of focal liver lesions on ultrasound images by extracting hybrid textural features and using an artificial neural network," *Bio-Med. Mater. Eng.*, vol. 26, no. s1, pp. S1599–S1611, Aug. 2015.
[24] R. Nair and B. Rost, "Better prediction of sub-cellular localization by combining evolutionary and structural information," *Proteins, Struct., Function, Bioinf.*, vol. 53, no. 4, pp. 917–930, Dec. 2003.

YING WANG received the Ph.D. degree in precision instrumentation and mechanics from the School of Instruments Science and Optoelectronic Engineering, Beihang University, Beijing, China, in 2006. From 2015 to 2016, she was a Visiting Scholar with Johns Hopkins University, USA. She is currently a Professor with the Institute of Microelectronics of the Chinese Academy of Sciences, Beijing. Her research interests include machine vision and image analysis.

LIN MAO received the bachelor's and master's degrees from the College of Information Science and Technology, Beijing University of Chemical Technology, Beijing, China, in 2013 and 2020, respectively. She currently works as an Engineer with the First Research Institute of the Ministry of Public Security of China, mainly engaged in medical image processing, pattern recognition, and deep learning.

MING-AN YU received the Ph.D. degree in imaging and nuclear medicine with People's Liberation Army Medical College, Beijing, China, in 2011. He completed postdoctoral work with the Cancer Center of Chinese People's Liberation Army General Hospital, in 2013. He is a Physician Associate Professor with the Department of Interventional Ultrasound Medicine, China-Japan Friendship Hospital, Beijing. His research interests include minimally invasive ablation and imaging diagnosis.

YING WEI received the master's degree in imaging and nuclear medicine from People's Liberation Army Medical College, Beijing, China, in 2013. She was a Visiting Scholar with Thomas Jefferson University, USA, in 2017. She is currently a Physician with the Department of Interventional Ultrasound Medicine, China-Japan Friendship Hospital, Beijing. Her research interest includes minimally invasive ablation of tumors.

CAN HAO received the bachelor's degree from Chongqing University, Chongqing, China, in 2015, and the master's degree from the School of Instrumentation and Optoelectronic Engineering, Beihang University, in 2018. She currently works as an Engineer with the Institute of Microelectronics, Chinese Academy of Sciences, mainly engaged in machine vision, image processing, and deep learning.

DENGFENG DONG received the Ph.D. degree in precision instrumentation and mechanics from the School of Instruments Science and Optoelectronic Engineering, Beihang University, Beijing, China, in 2012. He is currently an Associate Professor with the Institute of Microelectronics of the Chinese Academy of Sciences. His research interests include precision opto-electronics measurement, automation control, target recognition and tracking, and embedded system development.